5-1-1988

A. C. Power Losses in MOV Surge Arrestors

Alan J. Engelmann
Purdue University

W. L. Weeks
Purdue University

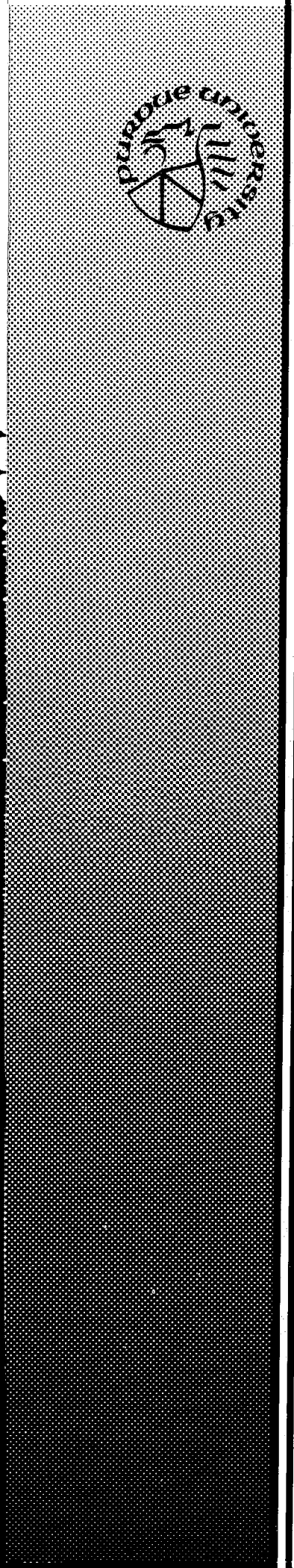

A. C. Power Losses in MOV Surge Arrestors

Alan J. Engelmann
W. L. Weeks

TR-EE 88-22
May 1988

School of Electrical Engineering
Purdue University
West Lafayette, Indiana 47907

A.C. POWER LOSSES IN MOV SURGE ARRESTORS

A study performed for
Purdue Electric Power Center

by
Alan J. Engelmann

advisor
W. L. Weeks

May 1988

1. Introduction

It was the objective of this study to measure power losses occurring in MOV surge arrestors as they were subjected to various voltage excitations. In particular, power losses were observed in two MOV devices as sinusoidal voltages of different magnitudes were applied, at various frequencies in the range of typical power frequencies and common harmonics. Power losses were also observed in an MOV device for applied voltages consisting of the sum of 60 Hertz sinusoids and a single harmonic.

The measurement procedure consisted of obtaining digital records representing the waveforms of voltage across and current through the MOV device during operation; power was calculated as the mean of the product of these digitally represented waveforms. This report contains a detailed description of the implementation of this procedure, as well as a discussion of some of its limitations when making measurements on highly reactive devices.

Experimental results indicate that power losses in the MOV devices studied were primarily dependent upon frequency of operation, and peak amplitude of applied voltage. The results indicate that 60 Hertz specifications given for a particular device do not, in general, apply for other frequencies or non-sinusoidal excitation.

2. Background

Metal Oxide Varistors (MOV) are ceramic devices which possess highly nonlinear V-I characteristics [1]. When a small voltage is applied to the device, it is virtually nonconductive. However, if the applied voltage is sufficiently high, the device begins to conduct. The voltage at which the device becomes significantly conductive is referred to as the breakdown, or turn-on voltage for the device. Once the turn-on voltage has been reached, the device will maintain a nearly constant voltage over a wide range of currents. These characteristics make the MOV device very useful in overvoltage protection applications. The devices also have the added advantage of being able to withstand high power operation, and thus are widely used as gapless surge arrestors in power applications [2].

For use as a surge arrestor, the device is operated at a level such that the system operating voltage is at some level sufficiently below the device turn-on voltage. Although virtually nonconducting at such an operating point, there is still a small conductivity associated with the device, and thus, a small power loss. It is this small power loss which this study investigates, and in particular, the effects that variations in operating voltage level and voltage waveform have upon this power loss.

3. Measuring Power Loss

Many standard power measurement techniques using conventional instrumentation require that current and voltage waveforms be sinusoids at standard power frequencies. The MOV, however, is a nonlinear device, and the current resulting from the application of even a sinusoidal voltage is not, in general, sinusoidal. Furthermore, this study entailed the application of voltage waveforms which were at frequencies other than 60 Hertz, and also non-sinusoidal waveforms. Thus it was required that an alternative approach be used.

For any two terminal passive device, having a voltage, $v_D(t)$, across its terminals and a current, $i_D(t)$, flowing through it, the instantaneous power consumed by the device is defined as

$$p_D(t) = v_D(t)i_D(t) .$$

The average power, P_{ave}, consumed by the device is the mean of $p_D(t)$. This approach could be physically implemented by digitally sampling $v_D(t)$ and $i_D(t)$, and calculating the mean of the product of the two waveforms. Such a method would allow power consumption to be determined regardless of voltage and current waveshape. Such was the approach taken in this study; a detailed description of the implementation of this procedure is contained in the following sections.

3.1 Single Frequency Measurements

It was the objective, in this first part of the study, to apply sinusoidal voltages of different magnitudes and frequencies, and observe the resulting power losses in an MOV device. In order to facilitate measurements, the MOV was incorporated into the circuit shown in Figure 3.1a of the appendix.

The magnitude of the voltage, $v_D(t)$, which was applied to the device was typically in the kilovolt range; the capacitive voltage divider, formed by C_1 and C_2, was used to provide a more easily measured quantity, $v_V(t)$, tenths of a volt in magnitude, from which $v_D(t)$ could be determined. Device current, $i_D(t)$, was obtained from the voltage, $v_I(t)$, across resistor R_I, which appears in series with the MOV device. The value of R_I was chosen small enough that the voltage drop across it could be assumed to be negligible in comparison to the voltage across the MOV device.

It should be noted that current flow through the MOV device increases substantially as the applied voltage approaches the turn-on level, and thus if the device is operated at a high enough voltage, current flow could increase to the point where $v_I(t)$ was no longer of negligible magnitude. In all power measurements described in this report, the MOV devices were operated at levels low enough that it was assumed $v_I(t)$ could be ignored. In the following analysis, the device voltage, $v_D(t)$, will be assumed to be identical to $v_S(t)$.

In order to protect the measurement instrumentation from possible exposure to high voltages, all measurements were made through buffer amplifiers. The two buffer amplifiers used to measure $v_I(t)$ and $v_V(t)$ were chosen such that they were nearly identical in phase response. Measurements corresponding to the device voltage and current would then be shifted identically in phase (assuming similar waveforms), thus preserving the phase angle between the two waveforms. The phase shift introduced by the buffer amplifier responses could thus be ignored in the power measurement procedure.

When the buffer amplifiers are introduced, their input impedances, R_A and R_B, appear in the circuit as shown in Figure 3.1b of the appendix. R_A appears in parallel with R_I and must be taken into account in the calculation of $i_D(t)$ from $v_I(t)$. With resistance R_B appearing in parallel with C_2, the transfer ratio between $v_V(t)$ and $v_D(t)$, assuming they are sinusoids, may be expressed as a complex, frequency dependent quantity:

$$\frac{V_V(j\omega)}{V_D(j\omega)} = \frac{j\omega C_1 R_B}{1+j\omega(C_1+C_2)R_B} , \qquad (3.1\text{-}1)$$

where $V_V(j\omega)$ and $V_D(j\omega)$ are representations of $v_V(t)$ and $v_D(t)$ in the frequency domain. One interpretation of (3.1-1) is that $v_V(t)$ is simply a scaled and phase shifted version of the sinusoidal $v_D(t)$, with $v_V(t)$ leading $v_D(t)$ in phase. This implies that $v_D(t)$ may be obtained from $v_V(t)$ by advancing the waveform in time and magnifying its amplitude by a constant scale factor.

It should be noted here that an applied sinusoidal voltage will be significantly distorted if it drives the MOV device into its turn-on region; in particular, the peaks of the waveform will be suppressed. In this case, equation (3.1-1) and the subsequent analysis would not be accurate. In all power measurements described in this part of the report, the MOV devices were operated at low enough levels such that sinusoidal waveforms could be assumed.

Referring to Figure 3.1b, the quantities which were physically measured were $v_A(t)$ and $v_B(t)$. These waveforms were digitally sampled, and a record of samples was obtained, representative of at least one period of the applied voltage waveform. Note that the angular resolution of the data record is dependent upon the sampling rate. If, for example, a sinusoidal waveform, $x(t)$, of frequency f_o Hertz were to be sampled, over one period, at a rate of f_s samples per second, then the number of samples obtained for that one period of $x(t)$ would be

$$n_p = f_s/f_o . \qquad (3.1\text{-}2)$$

The angular spacing between consecutive samples would be, in degrees,

$$\Delta\Theta = 360/n_p = 360f_o/f_s \ . \qquad (3.1\text{-}3)$$

It was desirable, in this application, that $\Delta\Theta$ be small so that phase correction could be precisely made. For a given f_o, this is accomplished by increasing f_s.

After acquiring the sample records of $v_A(t)$ and $v_B(t)$, the data was scaled in magnitude and corrected in phase such that accurate representations of the device voltage and current were obtained. A record of the device current, $i_D(t)$, was obtained by dividing the $v_A(t)$ data by a quantity equal to the combined parallel resistance of R_I and R_A, and also dividing out the gain of the buffer amplifier. In obtaining a record of $v_D(t)$, magnitude scaling of the $v_B(t)$ measurements was achieved by simple multiplication of the data by a frequency dependent scale factor. Phase correction, also a frequency dependent quantity, was accomplished by shifting the data by an appropriate number of points within the data record. In order to shift positively in phase by Θ_s degrees, the data was shifted

$$n_s = \frac{\Theta_s f_s}{360 f_o} \qquad (3.1\text{-}4)$$

samples forward within the data record, where f_s and f_o represent sampling rate and frequency of the applied waveform, as before. The exact magnitude and phase corrections necessary are determined by equation (3.1-1) and buffer amplifier gain. These scaling factors were also checked experimentally.

Having performed the above manipulation of the data, the digital records representing $i_D(t)$ and $v_D(t)$ were multiplied point for point, yielding a discrete representation of the instantaneous power waveform, $p_D(t)$. Calculating the mean of this product over an integral number of periods provided an estimate of the average power consumed in the device.

3.2 Multiple Frequency Measurements

In this part of the study, it was desired to observe power losses when the applied voltage waveform consisted of the sum of a 60 Hertz sinusoid and a single harmonic. Measurements were to be taken for different magnitudes of both the 60 Hertz fundamental and the harmonic, and also for different frequency harmonics.

If a capacitive voltage divider were to be used for these measurements, a simple shift along the time axis would not restore the original phase characteristics of the voltage waveform, as in the single frequency measurements of section 3.1, since there are now two distinct frequencies present in the signal. Having knowledge of the transfer characteristics of the circuit, the original waveform could be recovered using more advanced digital signal processing techniques; however, it was decided to use a resistive voltage divider for simplicity. Although, in some applications, high voltage resistive dividers have some problems associated with parasitic impedances [3,4], frequencies were low enough that it was assumed that the divider could be considered purely resistive.

The circuit used in this series of measurements was identical to that used in the single frequency measurements (Figure 3.1b), except that capacitors C_1 and C_2 were replaced by two resistors. Power calculations were performed as described in section 3.1, except that magnitude scaling of $v_B(t)$ was assumed to be independent of frequency, and no correction was performed for phase.

3.3 Effect of Phase Angle on Accuracy

Recall that for a linear device, power consumption may be related to the phase angle, Θ, between voltage and current as

$$P_{ave}(\Theta) = V_{rms} I_{rms} \cos\Theta \,, \tag{3.3-1}$$

where V_{rms} and I_{rms} are the r.m.s. values of sinusoidal voltage and current waveforms applied to the device [5]. Thus for constant V_{rms} and I_{rms}, average power varies as $\cos\Theta$.

Now consider the effect a small perturbation, δ, has on the value of $P_{ave}(\Theta)$:

$$P_{ave}(\Theta+\delta) = V_{rms}I_{rms}\cos(\Theta+\delta) .$$

Note that when Θ is small, $d/d\Theta\ \{\cos\Theta\} = \sin\Theta$ is at a minimum; therefore $P_{ave}(\Theta)$ changes very little for a small perturbation in Θ. As Θ approaches 90°, however, $d/d\Theta\ \{\cos\Theta\}$ reaches a maximum, and a small perturbation in Θ results in a much larger change in $P_{ave}(\Theta)$. If the perturbation, δ, represents an error in the phase angle between a voltage and a current waveform, and the product of the two is used in the calculation of average power (as described in previous sections), then the resulting error in the power calculation may be represented as

$$\text{Error}(\Theta,\delta) = 1 - \frac{P_{ave}(\Theta+\delta)}{P_{ave}(\Theta)} . \qquad (3.3\text{-}2)$$

A plot of this relationship for several small negative values of δ is shown in Figure 3.3a of the appendix. A positive δ would produce a similar effect. Note the dramatic increase in error with respect to angle as Θ approaches 90°.

This relationship of error to phase angle places limitations on the accuracy which can be expected in the power measurement procedures described in the previous sections when the phase angle between voltage and current is large. For example, a small inaccuracy in the phase correction factors for the capacitive voltage divider described in section 3.1 could result in disproportionately large errors in the power calculation. Similarly, large errors would arise in measurements obtained using the resistive divider of section 3.2 if parasitic reactances in the resistors produced an adequate amount of phase shift. These results are significant because the MOV is highly capacitive when operating below turn-on, and therefore the phase angle between voltage and current will tend to be quite large.

Note also that the procedure of 3.1 (capacitive divider) involves a discrete phase correction, and the precision to which this correction can be made, even if the necessary angular compensation is exactly known, is limited by the angular resolution, which was referred to as $\Delta\Theta$ in (3.1-3). Assuming the correction is made to the nearest data point, the greatest angular error, δ, which is possible is $\pm$ 1/2 $\Delta\Theta$, or from the expression for $\Delta\Theta$ in (3.1-3),

$$\delta = \pm 180 f_o/f_s = \pm 180 f_o T_s \qquad (3.4\text{-}3)$$

degrees, where T_s is the sampling period, $1/f_s$. δ may be decreased by increasing the sampling rate, f_s, but there are limitations on how fast one can sample. Also, if the collected data is to represent at least one period of the applied waveform, more data must be stored as f_s is increased, requiring that more memory be available, and with more data points representing the waveforms, more mathematical operations are involved in processing the data, resulting in increased calculation time.

When the phase angle between voltage and current is very high, greater accuracy may be achieved by placing a known resistance in parallel with the MOV device, and then performing a power measurement for the parallel network. The phase angle of the parallel network is less than that of the MOV alone, and so the accuracy of the measurement is increased. Power loss in the resistor may then be calculated as V^2/R and subtracted from the net power to yield power loss in the MOV device alone. This technique was found to be very useful in making power measurements at higher phase angles, where the slope of the error versus angle relationship becomes very steep.

4. Experimental Results

Digital measurements and numerical processing were performed with a Data 6000 waveform analyzer unit, which was programmed to perform the power calculation procedures. Typically, several measurements were made consecutively, and the results averaged to obtain the final result. The number of samples used in each data acquisition was 2048, chosen on the basis of available memory resources. Sampling speeds were such that the

minimum number of points per period was around 1400. From (3.1-3), this corresponds to an angular resolution of at least $\Delta\Theta = 360°/1400 = 0.257°$. High voltage waveforms were obtained using a Behlman 6000 VA A.C. power supply, the output of which was stepped up using a small 10 kVA distribution transformer.

4.1 Single Frequency Measurements

Two devices, each from different manufacturers, were tested. They will be referred to as sample A and sample B. Physically, both devices were discs, possessing an outer diameter of 2 inches and a thickness of 3/4 inch. 60 Hertz specifications for device A indicated a current flow of 1mA (presumably peak value), with an applied voltage of 3230 volts, peak amplitude. Specifications for device B were 10.4mA, peak, at 3680 volts, peak.

The resistors and capacitors used in the measurement circuit, Figure 3.1b, were measured under low voltage conditions to within 1%. Current sensing resistor R_I was 93Ω. Input impedances of the buffer amplifiers, R_A and R_B, measured slightly more than 2KΩ. C_2, the low voltage element of the voltage divider, was 0.94μF; the high voltage element, C_1, was an oil-filled, high-voltage capacitor measuring 96pF.

Scaling factors computed for the voltage divider based on the above values were checked experimentally. Magnitude scaling was checked by use of a digital network analyzer, and was found to be accurate to within 1%. Phase correction factors were checked by taking measurements with the MOV in the measurement circuit replaced by a high-voltage resistor, and using the calculated correction factors to generate records of $v_D(t)$ and $i_D(t)$. The two digitized waveforms were then displayed, and it was visually ascertained that the phase difference between the two was zero. At several frequencies, the phase difference between the two records did not appear to be exactly zero; the correction factor used in the MOV measurements was that which experimentally aligned the two signals. The greatest error observed was at 60 Hertz, where $i_D(t)$ appeared to lead $v_D(t)$ by about 2°.

Power losses were observed for the two devices for applied sinusoidal voltages which were 35%, 50%, 70%, and 80% of the manufacturer specified turn-on voltage, and at frequencies between 60 and 1020 Hertz. Average power losses measured for the two devices have been plotted versus frequency in Figures 4.1a and 4.1b.

It was noted that the turn-on characteristics of the devices were somewhat frequency dependent. Plotted in Figure 4.1c are the peak values of applied sinusoidal voltages which were found to cause a peak current of 10 mA through the devices at several different frequencies.

Also included in the appendix, in Figures 4.1d through 4.1k, are plots of instantaneous voltage, current, and power waveforms resulting in a few of the single frequency tests. It should be noted that the small spikes appearing in the current waveforms (and consequently in the power waveforms as well) were produced by the power supply, and are not a characteristic of the MOV's conduction. Also included for illustration, in Figure 4.1l, are similar plots for device A as it is just beginning to turn on, and, in Figure 4.1m, for a slightly higher applied voltage.

4.2 Results For Added Harmonics

In this portion of the experiment, two synchronized, single frequency sinusoids, one at 60 Hertz and one at an odd harmonic frequency, were mixed together to produce a voltage waveform. The harmonic signals were aligned with the 60 Hertz sinusoid such that positive zero crossings would be coincident in time, i.e., the two signals, when added together, would have constructive peaks. The signal was constructed by additively combining the outputs of two synchronized waveform generators. The device tested was sample A, as used in the single frequency measurements.

The values of R_I, R_A, and R_B were 93Ω, 2KΩ, and 2KΩ, as before. As for the resistive divider components, the low-voltage resistor was 500Ω, and the high-voltage resistor measured 9.7MΩ, within 1%.

In the first series of measurements, the 60 Hertz fundamental was kept at a constant magnitude, while the harmonic component was increased in magnitude from zero until the device was near turn-on. Measurements were performed for fundamental component voltage magnitudes 50% and 70% of turn-on, and for 3rd, 5th, and 7th harmonics. Results are plotted in Figures 4.2a and 4.2b.

In the second series of measurements, the peak voltage of the 60 Hertz/harmonic combinations were to be kept constant, but the frequency of the harmonic component was varied. For one set of measurements, the 60 Hertz component had magnitude 50% of the turn-on voltage; in a second set of measurements, the 60 Hertz component had magnitude 70% of turn-on. In both cases, however, the harmonic components were of magnitude such that, when added to the 60 Hertz components, the resulting waveforms had peak values equal to 80% of the device turn-on voltage. Thus, both waveforms had identical peak voltages, but the magnitudes of the frequency components were of different proportion. Results from this series of measurements are plotted in Figure 4.2c, for harmonic frequencies between 180 and 1020 Hertz.

Plots of instantaneous voltage, current, and power waveforms are included for this series of measurements also, in Figures 4.2d through 4.2e.

4.3 Discrepancy Between the Two Experiments

It should be noted that a discrepancy was observed between results obtained using the capacitive voltage divider and those obtained by use of the resistive voltage divider. In particular, the results obtained for the additive harmonic experiments, which used a resistive divider, when the harmonic was of zero magnitude (the waveform was a 60Hz sinusoid) were around 25% lower than the power losses calculated in the single frequency measurements at 60 Hertz for the same device, where the capacitive voltage divider was employed.

Circuit element values were too well known for the error to have been a result of inaccurate magnitude scaling, thus the possibility of phase errors, as discussed in section 3.3, were examined.

The phase angle between MOV voltage and current for the 60Hz measurements was measured to be 80°. From (3.3-2), this implies that the phase error would have to be about 2° too large if the resistive divider were at fault. The possibility that parasitic reactance in the resistive divider could cause such a phase shift was investigated; however, it was found that the magnitudes of these reactances would have to be enormous in order to produce the 2° phase shift.

Turning to the capacitive divider, (3.3-2) reveals that a phase angle 2° smaller than anticipated, or equivalently, a phase correction factor 2° too large, could cause the observed error. Conductance in C_1 was investigated, but was found to increase, rather than decrease, the phase angle in question. It was also determined that an inaccuracy of 7% in the value of C_2 could cause this magnitude of error, but it is unlikely that the measurement of this component was so inaccurate. Finally, the error was traced to the use of the experimentally obtained phase correction factor, rather than the theoretically calculated one. Recall from section 4.1 that a 2° discrepancy arose in checking the phase correction at 60 Hertz experimentally. Use of the experimentally obtained result would account for the 2° excess in the phase correction factor. Error in the experimental result is suspected since it is known to have been erroneous in at least one other measurement (which was removed from the results given in this report); inaccuracy in the experimental phase measurement was most likely a result of not properly aligning the data records during the visual inspection procedure, as described in section 4.1.

5. Discussion

Upon observation of the single frequency measurements, plotted in Figures 4.1a and 4.1b, it is obvious that, in the frequency range observed, power loss in both MOV devices increases with frequency; upon a first approximation, this increase appears to be nearly linear. It is also noted that the slope of the curves increases as the magnitude of the applied voltage is increased. Figure 4.1c indicates that the turn-on voltage of the devices also apparently rises with frequency, which is possibly due to the device not having enough time to fully turn on at higher frequencies.

Figures 4.2a through 4.2c illustrate the power losses observed in an MOV device when the applied voltage was a 60 Hertz sinusoid with an added harmonic. In observing Figures 4.2a and 4.2b, peak applied voltage seems to be the prime influence on power loss, although a slight frequency dependency is apparent; this is indicated more clearly in Figure 4.2c. Losses appear to rise slightly for harmonics progressively higher than the 5th; this would be expected from the single frequency results. For the chosen peak voltage, the waveform which included the third harmonic caused the device to begin to turn on; hence the unexpectedly high value of power loss at the third harmonic, in comparison to higher harmonics. It was assumed that the device entered turn-on only for the third harmonic because of the lower turn-on voltage for this frequency. Figure 4.2c also shows that, of waveforms possessing equivalent amplitudes, the waveform containing the greater 60 Hertz component (curve ii) produced generally higher power losses, particularly at the lower frequencies. A curve from the single frequency data, labeled "S", was included in Figures 4.2a and 4.2b, and supports this trend, i.e., the pure 60 Hertz sinusoid produced a higher power loss than waveforms of equal amplitude, but containing a smaller low frequency (60 Hertz) component.

Note that in the figures referred to above, the discrepancy between the two experiments, as discussed in section 4.3, is apparent. Ideally, the first points of the "S" curves should coincide with the corresponding multiple frequency points. While this discrepancy is great enough to be perceptible, the comparison of the two data sets, nonetheless, should effectively demonstrate the observations described above.

In summary, power loss in the MOV devices studied appears to be highly dependent on operating frequency when sinusoidally excited. In the case where harmonics are present in a 60 Hertz sinusoidal voltage waveform, losses appear to be primarily influenced by the peak amplitude of the waveform, and only slightly affected by the frequency of the harmonic. On the whole, the data collected in this study demonstrates that 60 Hertz power specifications for these devices are not, in general, accurate for non-60 Hertz or non-sinusoidal operation. This is an important point which should be considered when designing an MOV device into a non-60 Hertz application.

References

[1] Levinson, L. M., and H. R. Philip, "The Physics of Metal Oxide Varistors," *Journal of Applied Physics,* Vol. 46, No. 3, pp. 1332-1341, March 1975.

[2] Sakshaug, E. C., J. S. Kresge, and S. A. Miske, Jr. "A New Concept In Station Arrester Design," *IEEE Transactions on Power Apparatus and Systems,* Vol. PAS-96, No. 2, pp. 647-656, March/April 1977.

[3] Bowdler, G. W., *Measurements in High-voltage Test Circuits,* Oxford: Pergamon Press, 1973.

[4] Schwab, A. J., *High-Voltage Measurement Techniques,* Cambridge: M.I.T. Press, 1972.

[5] Hayt, Jr., W. H., J. E. Kemmerly, *Engineering Circuit Analysis,* 3rd Ed., New York: McGraw-Hill, 1978.

APPENDIX

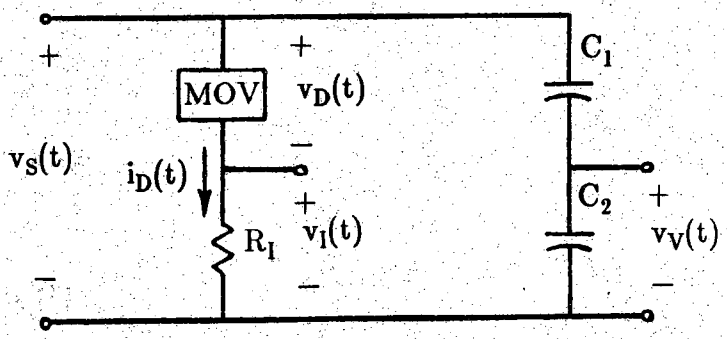

Figure 3.1a MOV measurement circuit configuration.

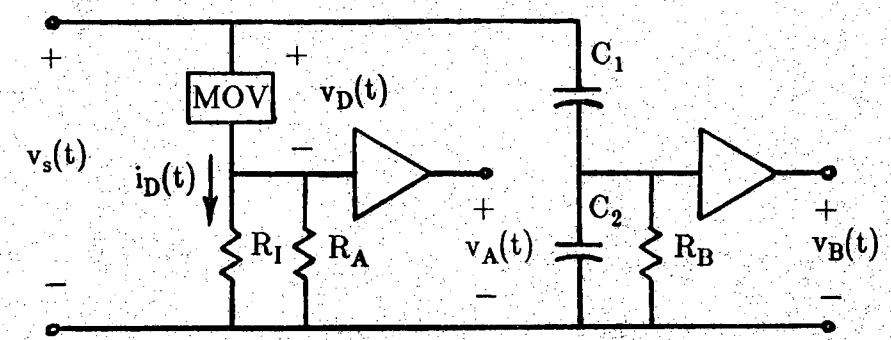

Figure 3.1b MOV measurement circuit, including buffer amplifiers.

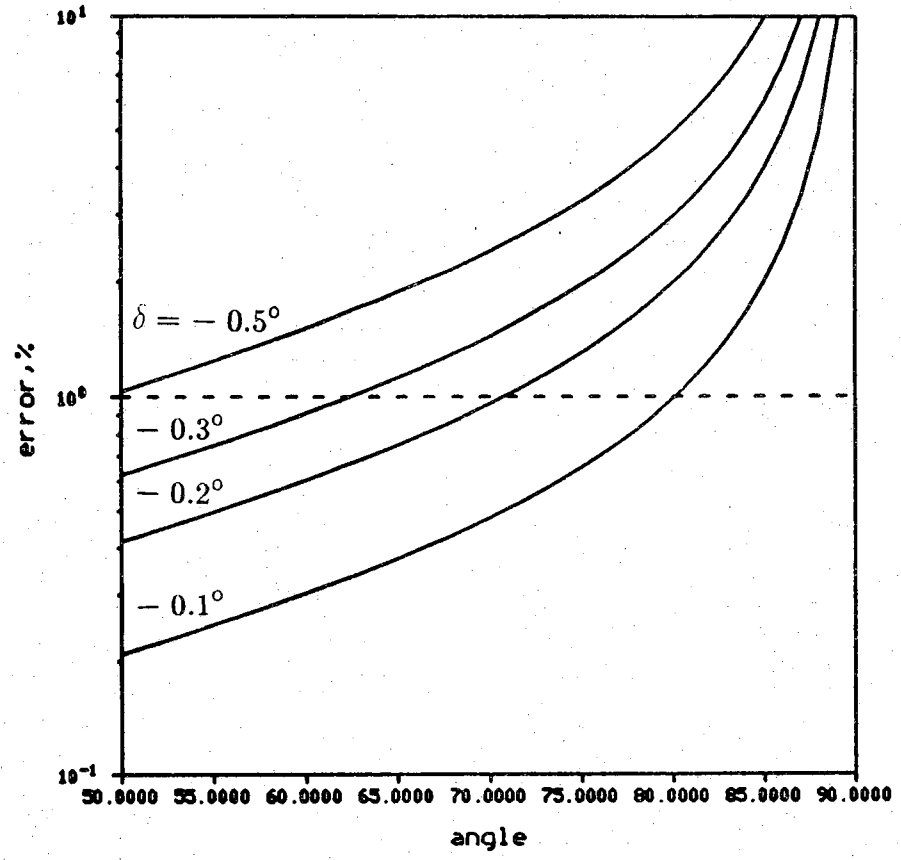

Figure 3.3a Percent error in power calculations resulting from several small perturbations in phase angle.

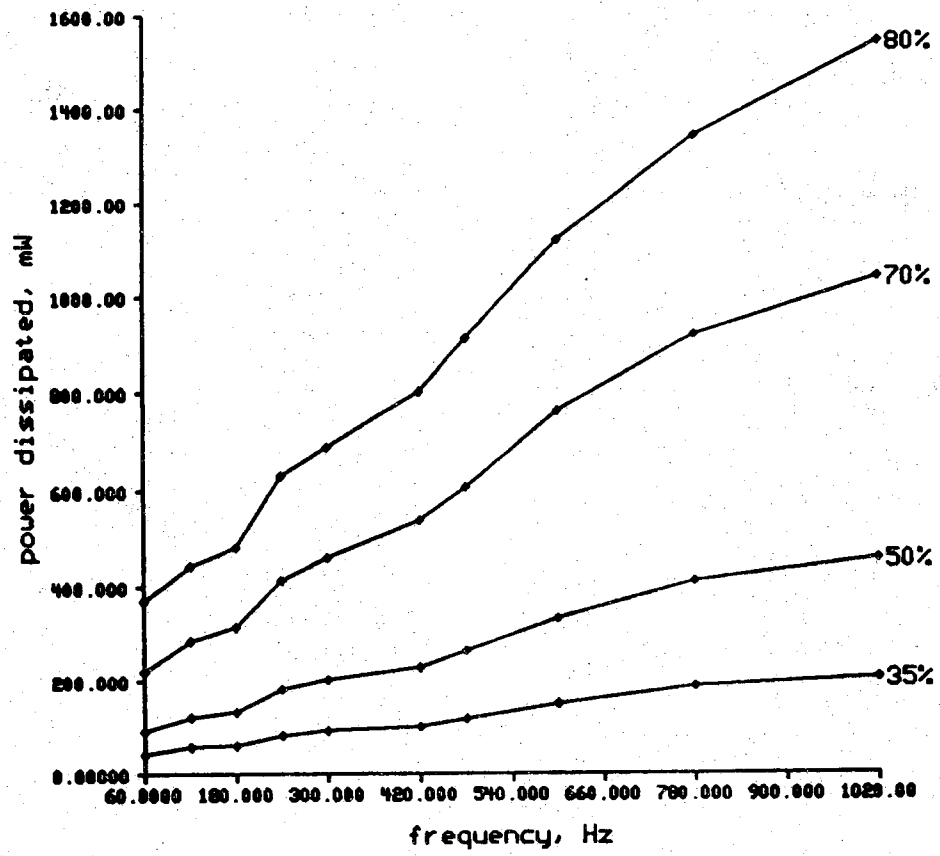

Figure 4.1a Single frequency power loss in sample A at 35%, 50%, 70%, and 80% of turn-on (3230 volts, peak).

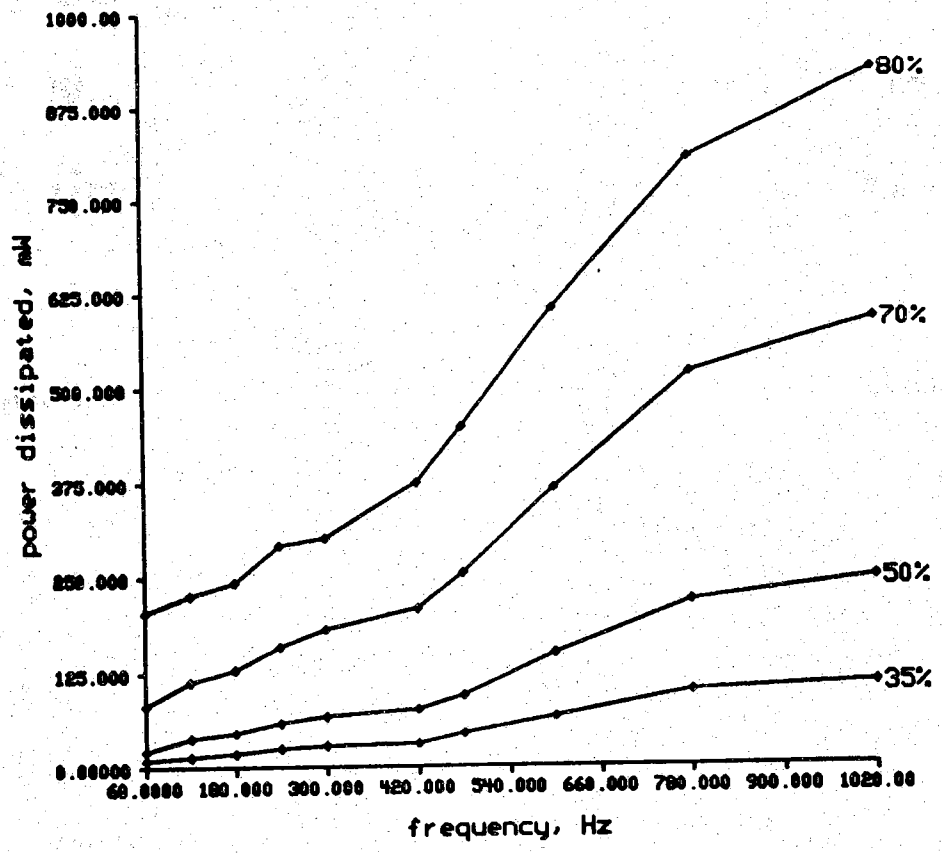

Figure 4.1b Single frequency power loss in sample B; turn-on at 3680 volts.

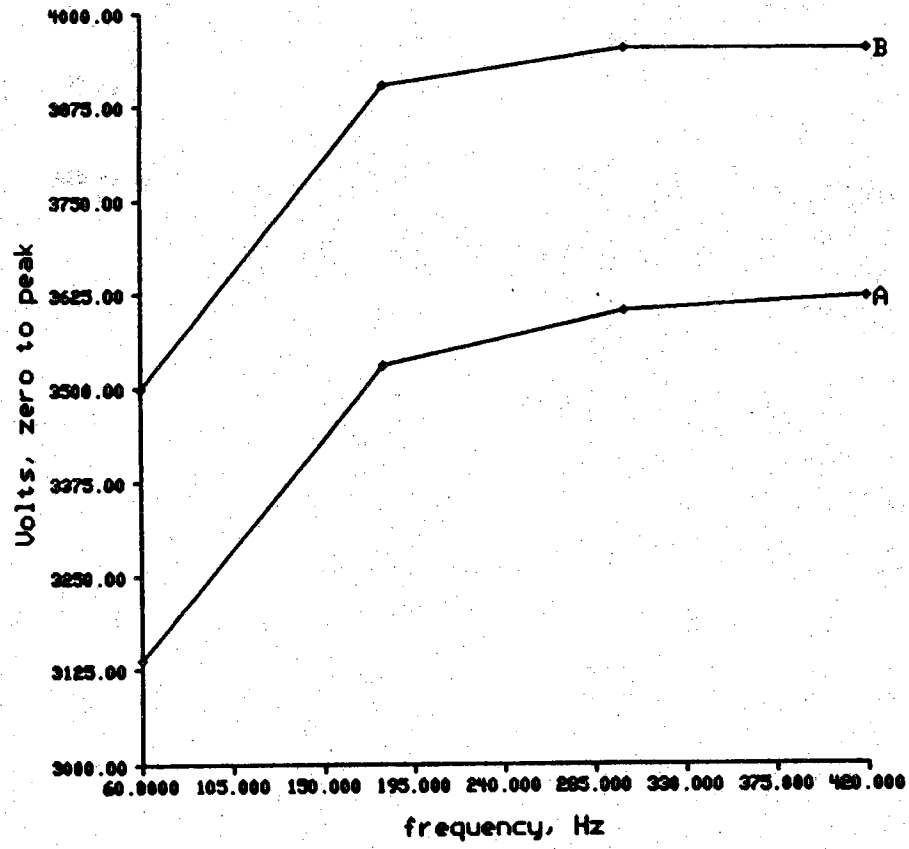

Figure 4.1c Sinusoidal voltages which produced peak currents of 10 mA in devices A and B.

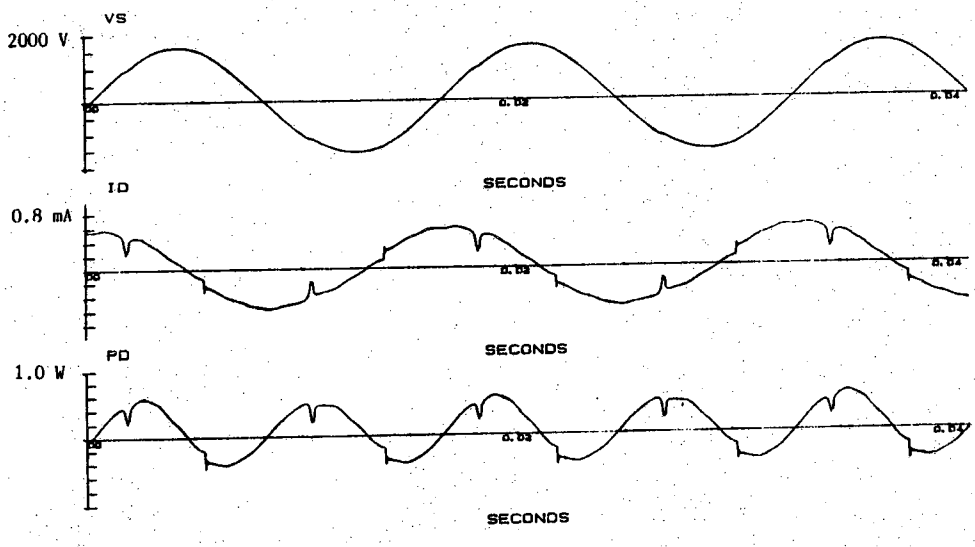

Figure 4.1d Sample A, operating at 60 Hz, 50% of turn-on.

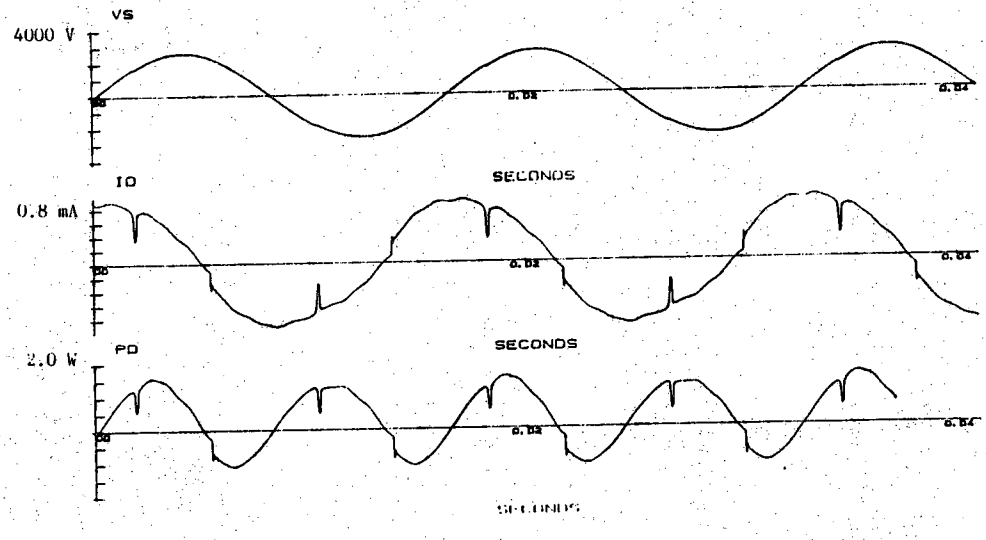

Figure 4.1e Sample A, operating at 60 Hz, 80% of turn-on.

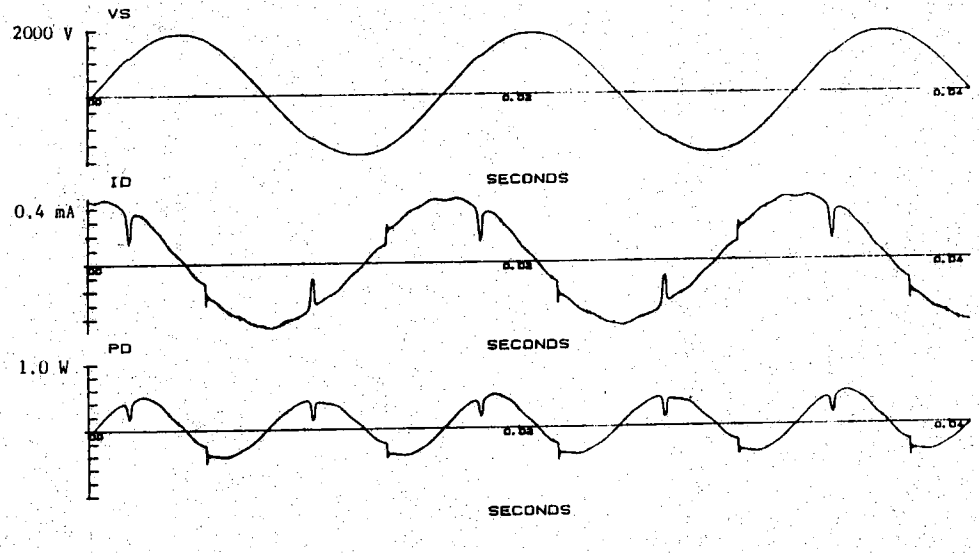

Figure 4.1f Sample B, operating at 60 Hz, 50% of turn-on.

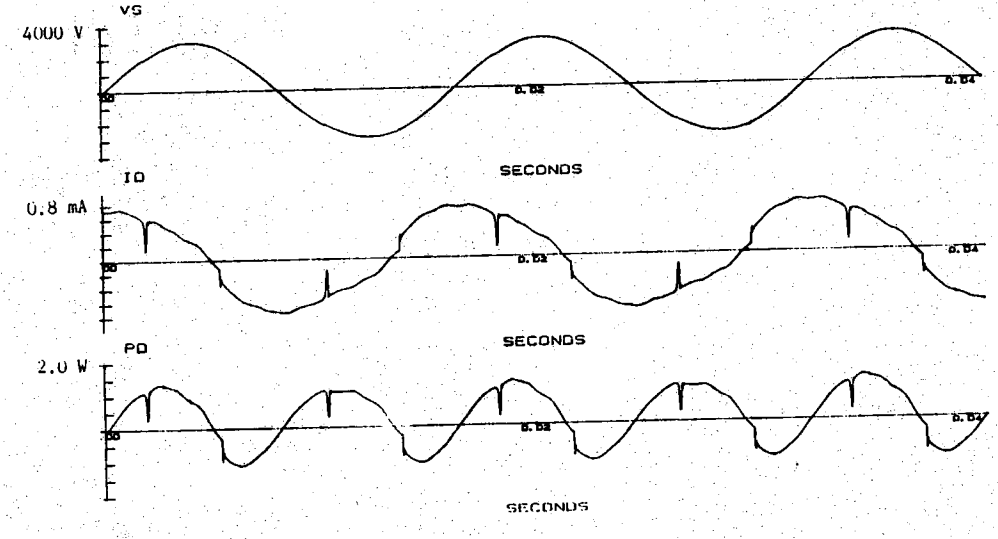

Figure 4.1g Sample B, operating at 60 Hz, 80% of turn-on.

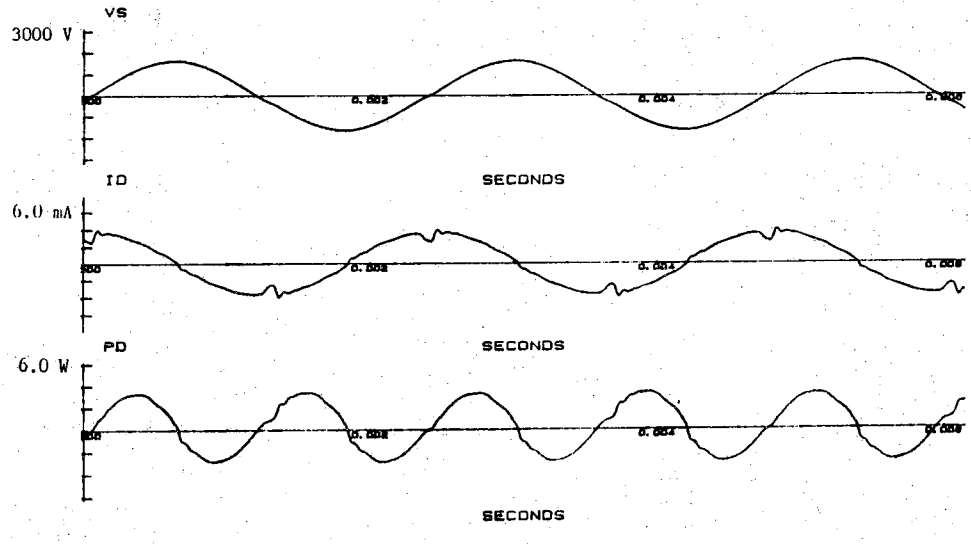

Figure 4.1h Sample A, operating at 420 Hz, 50% of turn-on.

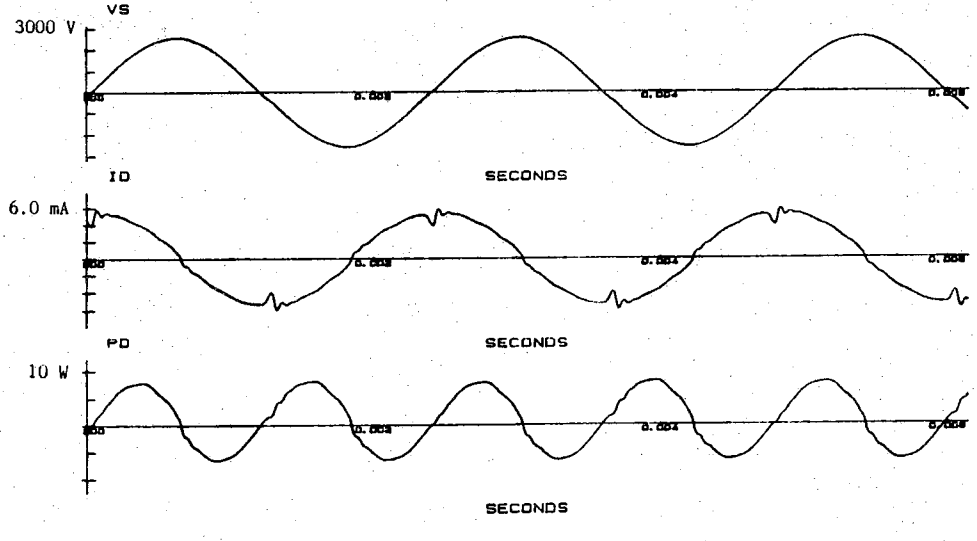

Figure 4.1i Sample A, operating at 420 Hz, 80% of turn-on.

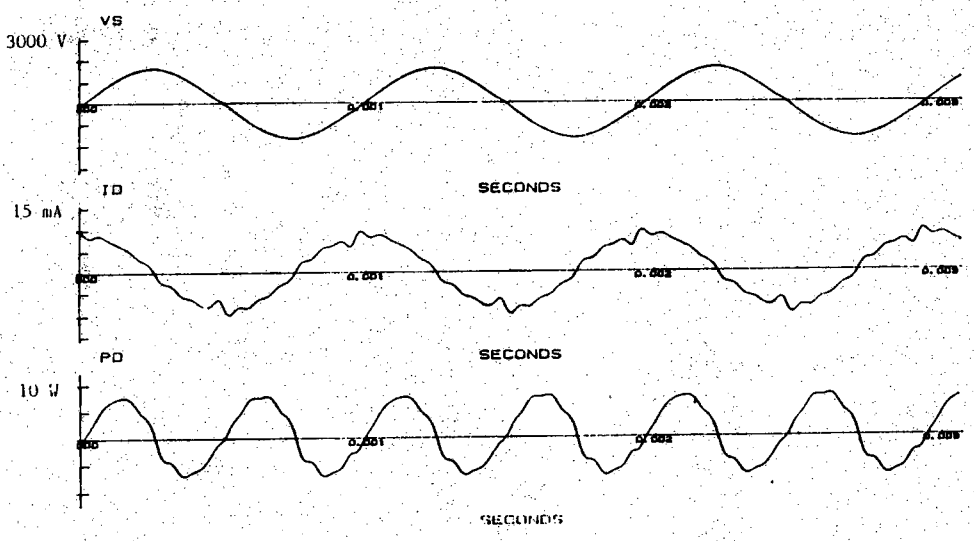

Figure 4.1j Sample A, operating at 1020 Hz, 50% of turn-on.

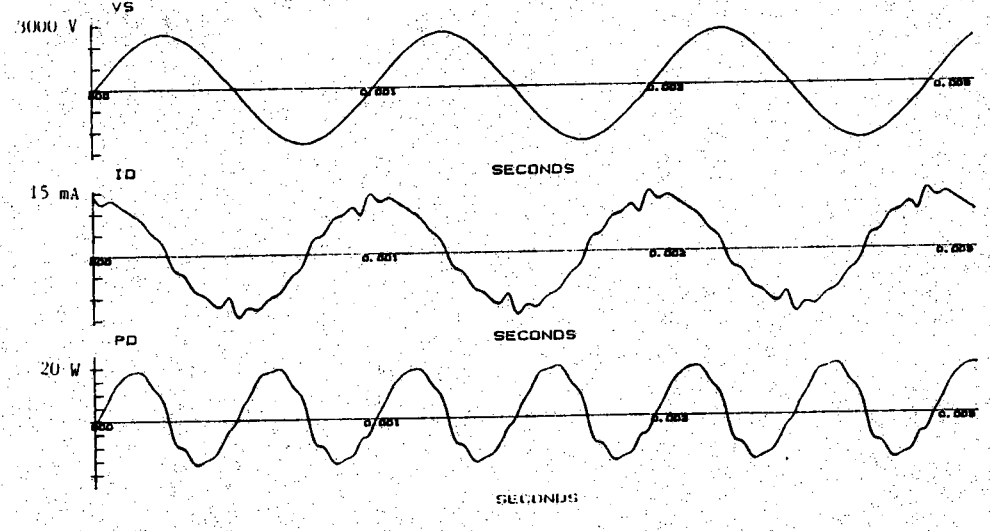

Figure 4.1k Sample A, operating at 1020 Hz, 80% of turn-on.

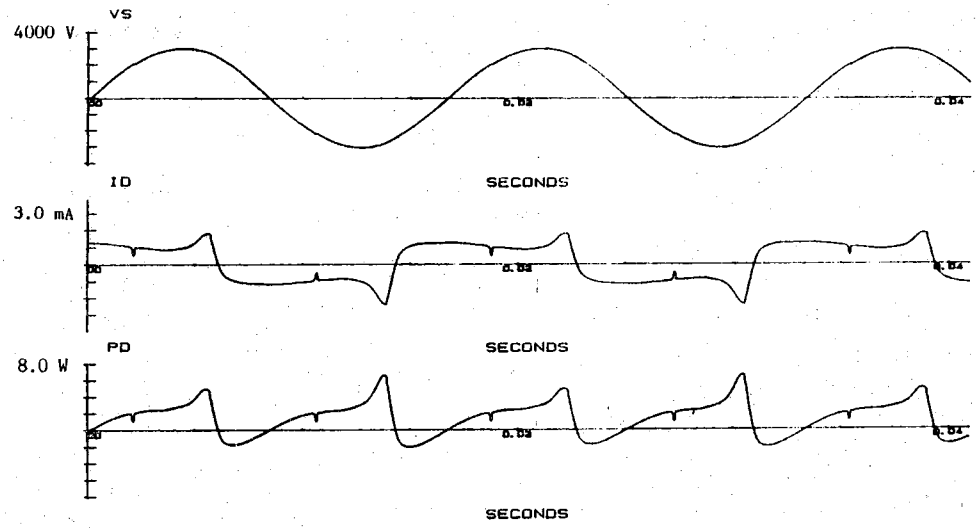

Figure 4.1l Sample A, beginning to turn on. V=2170 volts, rms.

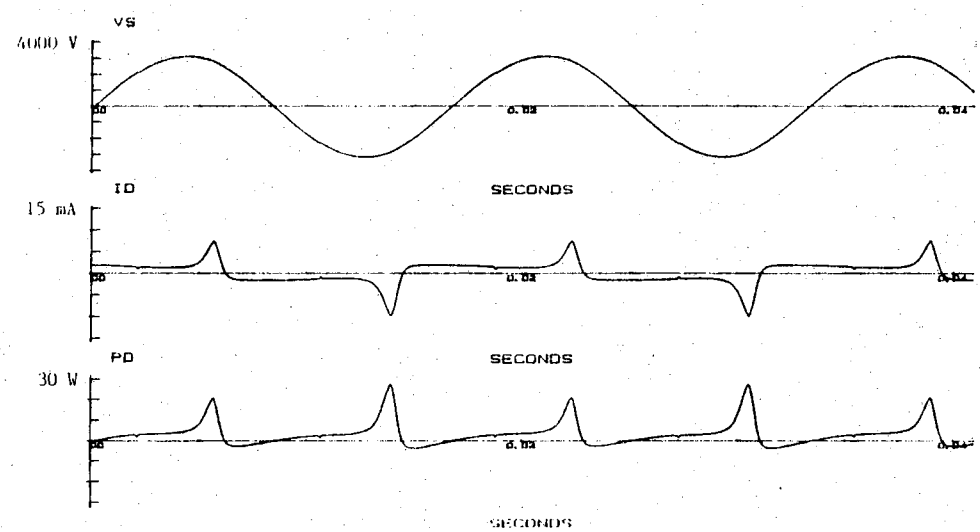

Figure 4.1m Sample A, at a slightly higher voltage. V=2200 volts, rms.

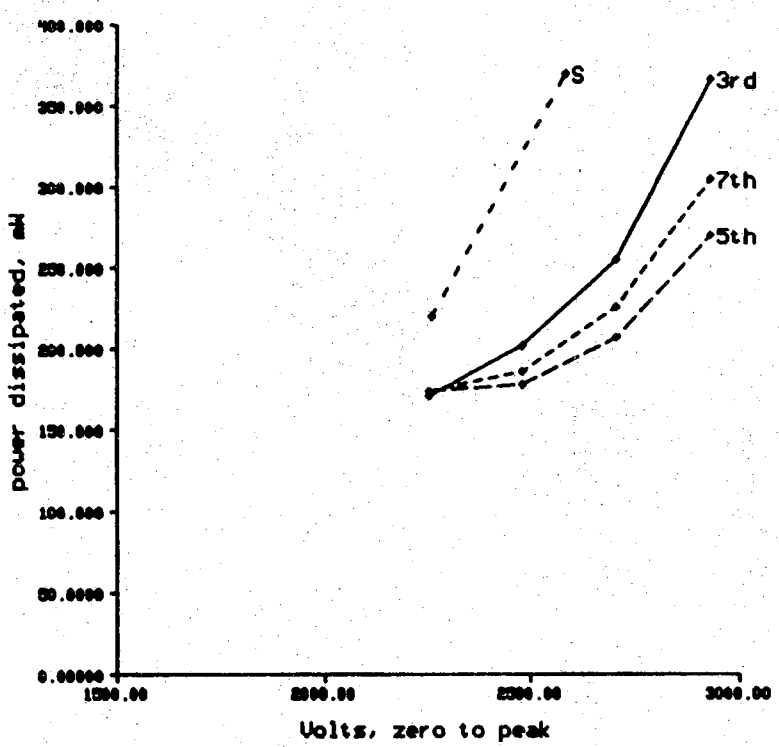

Figure 4.2a Power losses in sample A, 60 Hz component at 70% turn-on (3230 V).

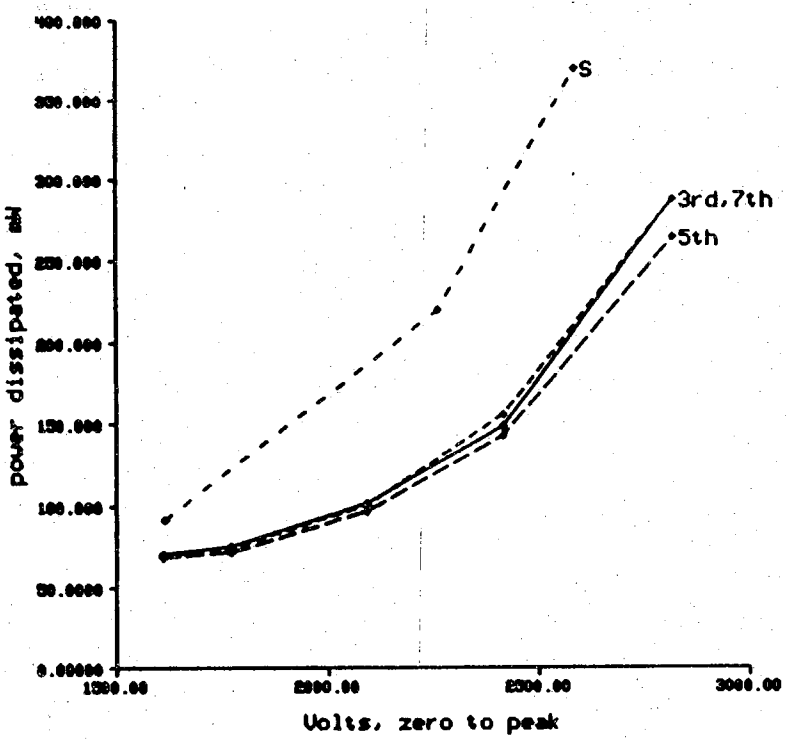

Figure 4.2b Power losses in sample A, 60 Hz component at 50% turn-on (3230 V).

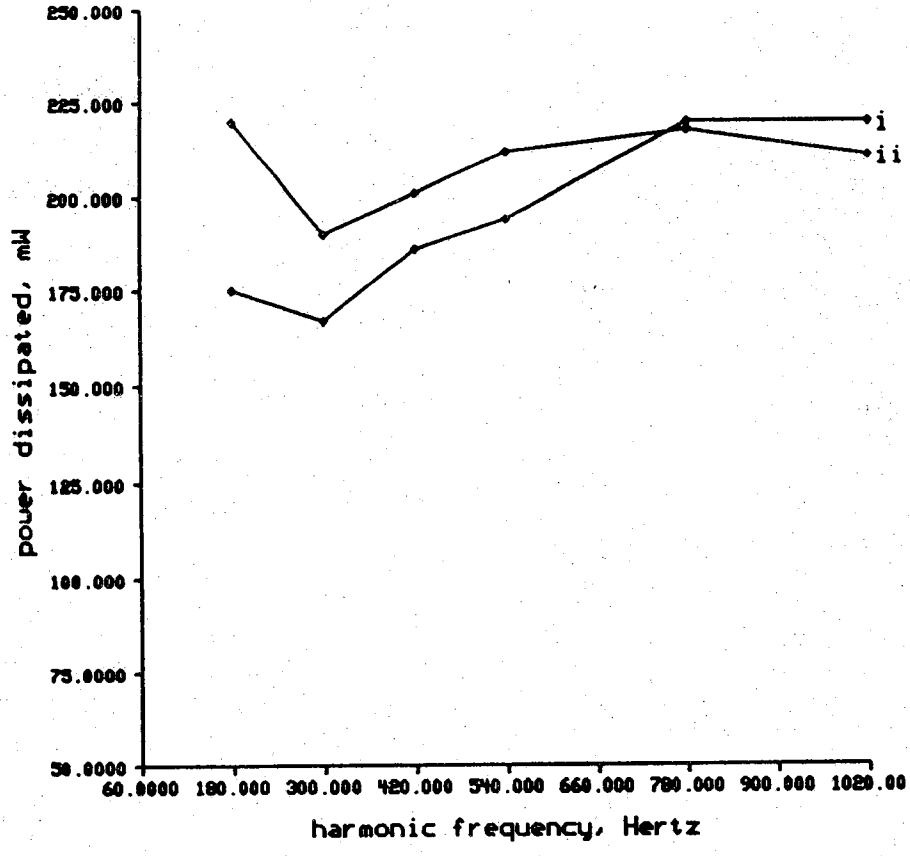

Figure 4.2c Power loss in sample A, peak voltage at 80% turn-on, 60 Hz component at i) 50% turn-on, and ii) 70% turn-on.

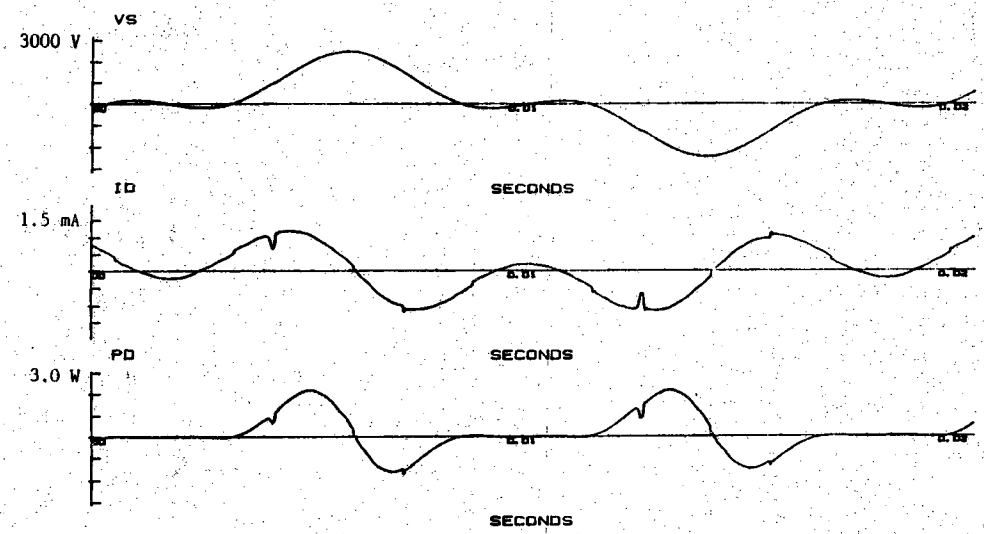

Figure 4.2d Sample A, 60 Hz component at 50%, added 3rd harmonic, peak voltage at 2420 V.

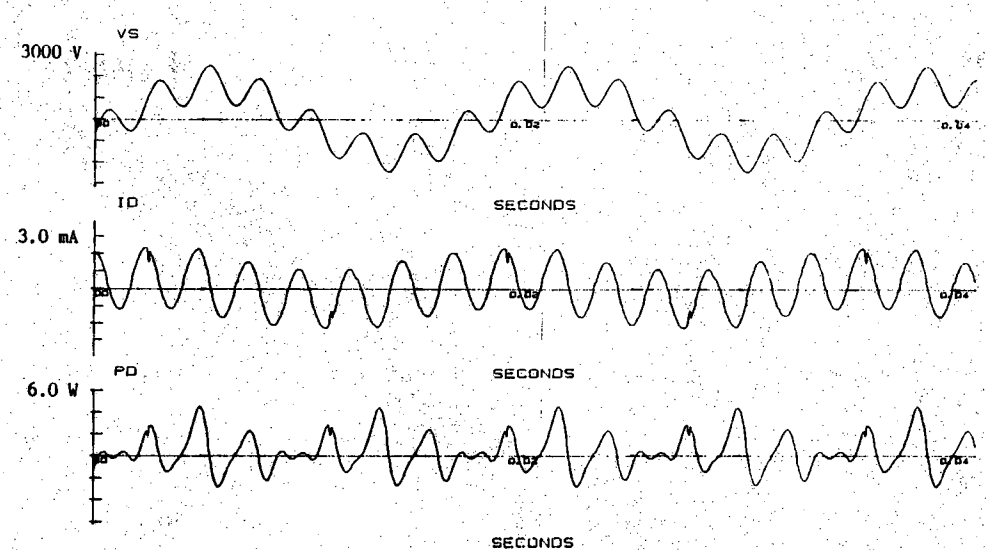

Figure 4.2e Sample A, 60 Hz component at 50%, added 7th harmonic, peak voltage at 2420 V.